Atmos. Chem. Phys. Discuss., 3, 389–411, 2003
www.atmos-chem-phys.org/acpd/3/389/

Atmospheric Chemistry and Physics Discussions

On the formation of radiation fogs under heavily polluted conditions

H. Kokkola, S. Romakkaniemi, and A. Laaksonen

Department of Applied Physics, University of Kuopio, Finland

Received: 1 November 2002 – Accepted: 17 January 2003 – Published: 3 February 2003

Correspondence to: H. Kokkola (harri.kokkola@uku.fi)

Abstract

We have studied the effect of gaseous pollutants on fog droplet growth in heavily polluted air using a model that describes time-dependent sulfate production in the liquid phase and thermodynamical equilibrium between the droplets and the gas phase. Our research indicates that the oxidation of SO_2 to sulfate has a significant effect on fog droplet growth especially when hygroscopic trace gases, for example HNO_3 and NH_3 are present. The increased sulfate production by dissolution of hygroscopic gases results from increased pH (caused by absorption of ammonia) and from the increased size of the fog/smog droplets. As a result of the enhancement of the droplet growth the optical thickness of the fog will increase.

1. Introduction

It has recently been shown that water-soluble gases that exist in high concentrations in polluted air, such as nitric acid (HNO_3), can increase the hygroscopicity of aerosol droplets as the gases dissolve into the aqueous phase (Kulmala et al., 1997; Laaksonen et al., 1998). Calculations have shown that at relative humidities slightly below 100% absorption of HNO_3 may lead to appearance of micron sized droplet populations indistinguishable from ordinary clouds or fogs. This can occur even though the droplets have not undergone the traditional activation process, i.e. the droplets have not passed their Köhler curve maxima.

Recent model calculations have shown that also NH_3 has a substantial effect on cloud droplet formation (Kulmala et al., 1998; Hegg, 2000). The simultaneous dissolution of NH_3 and HNO_3 and/or HCl in the droplets can significantly increase the hygroscopicity of aerosol droplets and decrease the critical supersaturation at the droplet surface.

It should be noted that there exists a precondition for the unactivated cloud formation, regardless of the pollution levels: the droplets must follow their equilibrium (Köhler)

curves very closely as they grow. With certain types of atmospheric clouds this would not be the case as the droplets are actually out of equilirium because of kinetic limitations in water vapor condensation (Nenes et al., 2001). Considering gases such as HNO_3, with mixing ratios orders of magnitude lower than those of water vapor, it is clear that the cooling has to be quite slow for the droplets to grow to micron size range retaining near-equilibrium all the time. Our preliminary cloud model calculations (Palonen, 2000) indicated that cooling rates on the order of 1 K/h at 278.15 K and 1000 mbar are required for the unactivated cloud formation to occur due to the uptake of HNO_3. Such cooling rates have been observed for radiation fogs (Roach et al., 1976).

The best known examples of radiation fogs formed at very polluted conditions were the infamous London smogs, which occurred during wintertime inversions. One of the features of these fogs was a very low visibility, at times only a few meters (Pearce, 1992). A low visibility hints at a high number concentration of relatively small droplets, and it is possible that at least a fraction of the London smogs were in fact unactivated fogs. Although it is clear that the low visibility was not caused by HNO_3 in this case, it has been reported that large amounts of hydrochloric acid was released in the air for example during the occurrence of the 1952 “killer” smog (Met Office, 2002), and indeed, HCl could be a partial cause of the low visibility. Another possibility is that heterogeneous sulfate production in unactivated droplets was the source of additional hygroscopic material which made them grow to the micron size range without activation.

The purpose of this study is to investigate the effects of sulfate production in growing, unactivated droplet populations when NH_3 and HNO_3 are present in the gas phase. Our focus is in the development of the size distributions and droplet chemical compositions as a function of time, and in the reduction of visibility. However, due to lack of chemical and thermodynamic data, we are not trying to model the London type smogs quantitatively. For example, we are using HNO_3 as a surrogate for HCl, the reason being that the available thermodynamic models suitable for our purposes account for HNO_3 but not for HCl. On the other hand, it has been shown that nitric and hydrochloric

acids have very similar effects on cloud formation (Kulmala et al., 1996). Furthermore, in our model the sulfate is produced in chemical reactions between dissolved sulfur dioxide and ozone. It is likely that during wintertime fog formation the ozone levels are generally quite low, and probably the sulfate production in the London smogs was mostly due to oxidation of SO_2 by O_2, catalyzed by metals. However, the catalyzed oxidation mechanisms are still quite poorly understood, and difficult to model in a reliable manner. We therefore describe the sulfate production simply by using the SO_2-O_3-mechanism at artificially high ozone levels (when compared to usual wintertime inversion conditions). Despite of these divergences from the real conditions, we believe that our model results reveal features of radiation fog formation under high pollution that are qualitative correct regardless of the actual sulfate production mechanisms and acidic gases involved.

2. Model for aqueous phase sulfate production

The model describes absorption of soluble gases by a polydisperse droplet population, and the production of sulfate due to oxidation of dissolved SO_2 in the droplets. The rate-limiting step is assumed to be the chemical reaction, and therefore we do not describe gas-phase diffusion in the model. Instead, the uptake of the gases is determined by requiring that Henry's law equilibrium holds in the beginning of each time step.

2.1. Thermodynamical model

The model to calculate the formation and the development of fog aerosol population is based on the inorganic aerosol thermodynamical equilibrium model AIM (Clegg et al., 1998). The AIM model determines activities, equilibrium gas partial pressures, and degrees of saturation with respect to solid phases in solutions containing water, and two or more of the ions (H^+, NH_4^+, NO_3^- and SO_4^{2-}) or (H^+, NO_3^-, SO_4^{2-}, Cl^- and Br^-) at temperatures from about 180 K to 330 K. In our calculations there are H^+, NH_4^+, NO_3^-

and SO_4^{2-} ions in the liquid phase.

Using the AIM model the molalities of NH_4^+, NO_3^- in each size bin were solved from Eqs. (1) and (2)

$$ {}^{m}K_{HNO_3} = \frac{\gamma_{NO_3^-} m_{NO_3^-} \gamma_{H^+} m_{H^+}}{p_{HNO_3}}, \quad (1) $$

$$ {}^{m}K_{NH_3} = \frac{\gamma_{NH_4^+} m_{NH_4^+}}{\gamma_{H^+} m_{H^+} p_{NH_3}}, \quad (2) $$

where ${}^{m}K_i$ ($mol^2 kg^{-2} atm^{-1}$) is the equilibrium constant, m_i ($mol\,kg^{-1}$) is the molality and γ_i is the molality based activity coefficient of solute species i, and p_{HNO_3} and p_{NH_3} (atm^{-1}) are the equilibrium partial pressures of nitric acid and ammonia at the surface of the droplet.

The charge balance requires that

$$ m_{H^+} = m_{NO_3^-} + 2m_{SO_4^{2-}} + m_{HSO_4^-} - m_{NH_4^+}. \quad (3) $$

Sulfate is assumed to be completely non-volatile, so the amount of water in droplets n_{H_2O} is calculated from equations

$$ S_{H_2O} = f^*_{H_2O} x_{H_2O} \exp\left(\frac{2\sigma v_{H_2O}}{RT r_p}\right), \quad (4) $$

where $f^*_{H_2O}$ is the mole fraction based activity coefficient of water, x_{H_2O} is the mole fraction of water, σ is the surface tension of the droplet calculated according to Martin et al. (2000), v_{H_2O} is the partial molar volume of water, R is the gas constant, T is the temperature and D_p is the droplet diameter.

Equations (1) to (4) are solved among all the size bins. The system is assumed closed and the species in all size bins are assumed to be in equilibrium between the liquid and gas phase. Thus, the partial pressures of dissolved gas and water at the droplet surface for all the size bins are equal to the partial pressures in the gas phase.

2.2. Oxidation of S(IV) to S(VI)

In the model, the gaseous phase includes NH_3, HNO_3, SO_2 and O_3. The gaseous SO_2 dissolves into the liquid phase according to the following dissociation reactions:

$$SO_2(g) \rightleftharpoons SO_2(aq), \tag{5}$$

$$SO_2(aq) \rightleftharpoons H^+ + HSO_3^-, \tag{6}$$

$$HSO_3^- \rightleftharpoons H^+ + SO_3^{2-}. \tag{7}$$

The equilibrium constants and their temperature dependencies are shown in Table 1.

Dissolved ozone reacts with liquid S(IV) producing sulfuric acid. To calculate the reaction rate we used the rate expression where all forms of dissolved S(IV) react with ozone (Seinfeld and Pandis, 1998)

$$\frac{d[\mathrm{S(IV)}]}{dt} = \{k_a[SO_2(aq)] + k_b[HSO_3^-] + k_c[SO_3^{2-}]\}[O_3]. \tag{8}$$

The reaction coefficients and their temperature dependencies are shown in Table 2.

The liquid phase diffusion and the gas phase diffusion are assumed to be fast so the rate determining sub-process in the oxidation is assumed to be the chemical reaction. Accordingly, the concentrations of dissolved gases are uniform inside the droplets.

Ozone oxidizes sulfur dioxide slowly compared to for example hydrogen peroxide H_2O_2, so using it as an oxidant gives a lower amount of sulfate production in droplets but shows qualitatively the effect of sulfate production on droplet growth and visibility.

2.3. Visibility

The model also includes a module for calculating the effect of the droplet population on the visibility. The visual range x_v was evaluated as the distance at which a black object

ACPD
3, 389–411, 2003

has a standard 0.02 contrast ratio against a white background (Seinfeld and Pandis, 1998). The visual range for a given particle population was calculated from

$$x_v = \frac{3.912}{b_{ext}(\lambda)}, \tag{9}$$

where b_{ext} is the extinction coefficient for light with wavelenght λ (Seinfeld and Pandis, 1998).

The extinction coefficient was calculated from

$$b_{ext}(\lambda) = \int_0^{D_p^{max}} \frac{\pi D_p^2}{4} Q_{ext}(m, \lambda, D_p) n(D_p) dD_p, \tag{10}$$

where Q_{ext} is the extinction efficiency and m is the refractive index of the particles. The calculation of extinction coefficient is presented in detail by Bohren and Huffman (1983). The refractive index for the particle was assumed constant at $m = 1.5 - 0.03i$ for all the size bins.

3. Model calculations

We made calculations for typical meteorological conditions of wintertime smog episodes. The smog episodes usually occur when there is a temperature inversion and low wind speed. The temperature inversion prevents vertical convection of gases and the low horizontal flow is not sufficient enough to remove the air pollution, so the air pollution is trapped in the atmosphere's lowest layer. In the calculations the system for the trace gases is assumed closed.

We made five runs for different combinations of gas phase pollutants to compare how different mechanisms affect the size distribution.

In all the runs we applied a log-normally distributed ammonium sulfate [$(NH_4)_2SO_4$] particle population. The geometrical mean diameter of the particles, D_p, was 200 nm

ACPD
3, 389–411, 2003

and the geometrical standard deviation of the population σ_{pg} was 1.5. The total number concentration of the particles was 1000 cm^{-3}. The distribution was split into 39 bins.

The temperature was decreased from 3 °C to 0 °C as shown in Fig. 1. As the temperature decreases, the relative humidity increases from 87% to 99.98% (Fig. 1).

The first run was without gas-phase pollutants so the growth of particles is basically according to the Köhler theory only with the difference that negligible amount of NH_3 originating from ammonium sulfate exits the droplets into the gas-phase.

In the second run, SO_2 and O_3 were introduced into the gas phase.

In the third run, there is HNO_3 and NH_3 in the gas phase. Now the growth of particles follows the modified Köhler curves. The dissolved pollutants increase the hygroscopicity of the droplets and enhance their growth.

In the fourth run, SO_2, O_3, HNO_3 and NH_3 are present in the gas-phase so there is a combined effect of increased hygroscopicity and sulfate production enhancing the growth of droplets.

The fifth run was otherwise similar as the fourth one, but there was no HNO_3 in the system.

The initial gas phase concentration for the trace gases were: $[SO_2]$ = 400 ppb, $[O_3]$ = 10 ppb, $[HNO_3]$ = 5 ppb and $[NH_3]$ = 10 ppb.

4. Results and discussion

Figure 2a shows the initial (t = 0 h) and final (t = 8 h) size distributions for clean air, while Figs. 2b–d compare the final size distributions in the polluted and clean cases.

In Fig. 2b, we can see that the presence of sulfate producing precursors SO_2 and O_3 slightly increase the size of droplets, especially the larger ones, also making the size distribution wider. The initial size distribution is almost exactly equal to the case of clean air, because dissolved SO_2 and O_3 have very little effect on the size of the droplets at 87% RH.

Figure 2c shows that the hygroscopic gases HNO_3 and NH_3 have a significant effect on the size of the droplets. For example, in this run, the largest size bin grows 1.5 times larger than in the case with no gaseous pollutants. HNO_3 and NH_3 affect the size distribution already in the beginning of the run. When HNO_3 and NH_3 coexist in the gas phase, their solubilities are increased, allowing them to dissolve in the liquid phase already at fairly low relative humidities.

Figure 2d shows the combined effect of hygroscopic gases and liquid phase sulfate production on the size distribution. The sulfate production further increases the size of the droplets and also makes the size distribution wider. In this run, the largest size bin grows 2.2 times larger than in the case of clean air. The initial size distribution in this case equals almost exactly the size distribution in Fig. 2c.

Figure 3 shows the amount of sulfate produced in the cases of Figs. 2b and d. The absorption of HNO_3 and NH_3 makes the droplets more hygroscopic, resulting in increased water vapor uptake and droplet volumes, which in turn facilitates increased sulfate production. The effect of gaseous pollutants on the total volume of the droplets can be seen in Fig. 4. HNO_3 and NH_3 cause the volume of the droplets to grow significantly. Sulfate production also enhances the hygroscopicity of the droplets, causing further growth of the droplets both in the presence of HNO_3 + NH_3 and in the presence of NH_3 alone. Ammonia is not very water soluble, and therefore, if nitric acid is excluded from the system, it is absorbed by the droplets only when enough of sulfate has been produced, in this case after about 1.5 h from the beginning of the run.

We also made a simulation with 15 ppb of HNO_3 and zero ammonia in the system. In this case, the droplet population grew as efficiently during the first 3 h as in the presence of nitric acid and ammonia; however, sulfate production was negligible due to low pH of the droplets. After 3 h the largest size class started growing very fast whereas the rest of the population stayed almost constant. This behavior may have been caused by a numerical artifact.

Figure 5 shows the gas phase concentrations as a function of time when all pollutants are present in the system. In the beginning of the run the gas phase concentration of

ACPD
3, 389–411, 2003

HNO_3 decreases as it partitions into the liquid phase. However, at about 4 h from the start the concentration starts to increase again due to the fact that the pH in the droplets decreases because of the sulfate production, driving nitric acid out of the droplets. Figure 6 shows the pH in the largest droplets as a function of time in the five cases considered. Sulfate production causes the final pH to approach 2.5. It has been estimated that in the London fogs, the pH was as low as 2 or even below.

To study the effect of enhanced sulfate production on the size distribution of the droplets, we made runs at very high ozone levels, and runs in which an increased reaction coefficient was applied. How these changes affect the total volume concetration can be seen in Fig. 7. In the beginning of the runs, the extra sulfate production increases the volume of the droplets. But as the pH of the droplets decreases as shown in Fig. 7, the production of sulfate decreases. Thus, at around 3,5 h from the beginning of the runs, the amount of hygroscopic matter, and thereby the sizes of the droplets, are roughly the same. Towards the end the pH of the droplets decreases in all the runs, and in the systems with higher sulfate production the droplets grow larger.

The visual range is shown as a function of time for four different runs in Fig. 8. The visual range was calculated at λ = 523 nm wavelength. The effect of HNO_3 and NH_3 can been seen already in the beginning of the run. For the two runs where there is no HNO_3 or NH_3 in the gas phase the visual range at the start of the run is 10038 m. This number drops to 5882 m when HNO_3 and NH_3 are present in the system.

After 8 h the visual range has decreased to 790 m in the clean air case. SO_2 and O_3 reduce the visual range to 748 m, and HNO_3 and NH_3 to 618 m. With all the trace gases SO_2, O_3, HNO_3 and NH_3 present in the system, the visibility is reduced to 521 m.

Comparing the results above with what is known about the London smogs, it is clear that our modelled visual range is too long and droplet pH too high. The visibility would be reduced by increasing the droplet concentration, and by accounting for interstitial aerosol and light absorbing components (soot). However, we believe that a more efficient sulfate production mechanism would also effect to reduce the visibility. As can be seen from Fig. 6 the pH-dependence of the oxidation of S(IV) by ozone is too steep

ACPD
3, 389–411, 2003

to allow for pH-values below 2 in the droplets. Furthermore, for technical reasons, the present calculations were carried out for a closed system. In reality, pollutants are often released continuously into the air when the smog is forming, and therefore it would be better to describe the smog formation in an open system. In such a case, the role of the soluble gases would probably be emphasized, and visibility would drop.

5. Conclusions

We have studied the effects of soluble gases and sulfate production on the formation and properties of radiation fogs. The effect of sulfate production alone on the droplet size distribution was rather modest; however, we applied the S(IV) oxidation mechanism by dissolved ozone, which is relatively inefficient especially at low pH values. Dissolved HNO_3 and NH_3 had a stronger effect on the size distribution, making it wider. This can be understood by noting that, due to a weaker Kelvin effect, larger droplets absorb soluble gases more effectively than do smaller ones.

The most significant finding of the work was that ammonia and nitric acid effectively boost sulfate formation in the droplets. Ammonia affects sulfate formation by keeping the droplet pH at a higher level than would otherwise be the case, whereas the additional effect of HNO_3 is caused by its hygroscopicity - the droplets take up more water due to absorption of nitric acid, and thus the total volume facilitating sulfate formation becomes larger.

In the future our goal is to use a cloud model with explicit description of gas-phase mass transfer of the different species. We will also include a sulfate production scheme that works at a lower pH than the O_3-mechanism, and study the effect of HCl on the sulfate production using an open system.

Acknowledgements. This work was supported by the Academy of Finland.

References

Bohren, C. F. and Huffman, D. R.: Absorption and scattering of light by small particles, John Wiley & Sons inc., 1983. 395

Clegg, S. L., Brimblecombe, P., and Wexler, A. S.: Thermodynamical model of the system H^+-NH_4^+-SO_4^{2-}-NO_3^--H_2O at tropospheric temperatures, J. Phys. Chem. A, 102, 2137–2154. 1998. 392

Hegg, D. A.: Impact of gas-phase HNO_3 and NH_3 on microphysical processes in atmospheric clouds, Geophys. Res. Lett., 27, 2201–2204. 2000. 390

Kulmala, M., Laaksonen, A., Aalto, P., Vesala, T., and Pirjola, L.: Formation, growth, and properties of atmospheric aerosol particles and cloud droplets, Geophysica, 32, 1–2, 217–233. 1996. 392

Kulmala, M. and Laaksonen A.: Charlson R. J., Korhonen P., Clouds without supersaturation, Nature, 388, 336–337. 1997. 390

Kulmala, M., Toivonen, A., Mattila, T., and Korhonen, P.: Variations of cloud droplet concentrations and the optical properties of clouds due to changing hygroscopicity: A model study, J. Geophys. Res., 103, 16183–16195. 1998. 390

Laaksonen, A., Korhonen, P., Kulmala, M., and Charlson, R. J.: Modification of the Köhler equation to include soluble trace gases and slightly soluble substances, J. Atmos. Sci., 55, 853–862, 1998. 390

Martin, E., George, C., and Mirabel, P.: Densities and surface tensions of $H_2SO_4/HNO_3/H_2O$ solutions, Geophys. Res. Lett., 27, 197–200, 2000. 393

Met Office: The Great Smog Of 1952, http://www.met-office.gov.uk/education/historic/smog.html, 2002. 391

Nenes A., Ghan S., Abdul-Razzak H., Chuang, P. Y. and Seinfeld, J. H.: Kinetic limitations on cloud droplet formation and impact on cloud albedo, Tellus, 53B, 133–149. 2001. 391

Palonen, V.: Formation mechanism of smog, M. Sc. Thesis, University of Kuopio, 2000 (in Finnish). 391

Pearce, F.: Back to the days of deadly smogs, New Scientist, 1850, 25–28. 1992. 391

Pruppacher, H. R. and Klett, J. D.: Microphysics of Clouds and Precipitation, Kluwer Academic Publishers, Netherlands, 1997.

Roach, W. T., Brown, R., Caughey, S. J., Garland, J. A., and Readings, C. J.: The physics of radiation fog: I – a field study., J. R. Met. Soc., 102, 313–333. 1976. 391

Seinfeld, J. H. and Pandis, S. N.: Atmospheric Chemistry and Physics, John Wiley & Sons inc., 1998. 394, 395, 402, 403

Table 1. Equilibrium coefficients (Seinfeld and Pandis, 1998)

Equilibrium	A (M or M atm^{-1})	B (K)
$SO_2(g) \rightleftharpoons SO_2(aq)$	1.2	10.48
$SO_2(aq) \rightleftharpoons H^+ + HSO_3^-$	1.3×10^{-2}	7.04
$HSO_3^- \rightleftharpoons H^+ + SO_3^{2-}$	6.6×10^{-8}	3.74
$O_3(g) \rightleftharpoons O_3(aq)$	1.3×10^{-2}	3.74

the temperature dependence is defined as
$K_{eq}(T) = A \exp\left[-B\left(\frac{1}{T} - \frac{1}{298\,K}\right)\right]$

Table 2. Reaction coefficients (Seinfeld and Pandis, 1998)

Reaction	A ($M^{-1}s^{-1}$)	B (K)	subscript
$SO_2(aq) + O_3(aq)$	2.4×10^4		*a*
$HSO_3^- + O_3(aq)$	3.7×10^5	5530	*b*
$SO_3^{2-} + O_3(aq)$	1.5×10^9	5280	*c*

the temperature dependence is defined as
$k(T) = A \exp\left[-B\left(\frac{1}{T} - \frac{1}{298\,K}\right)\right]$

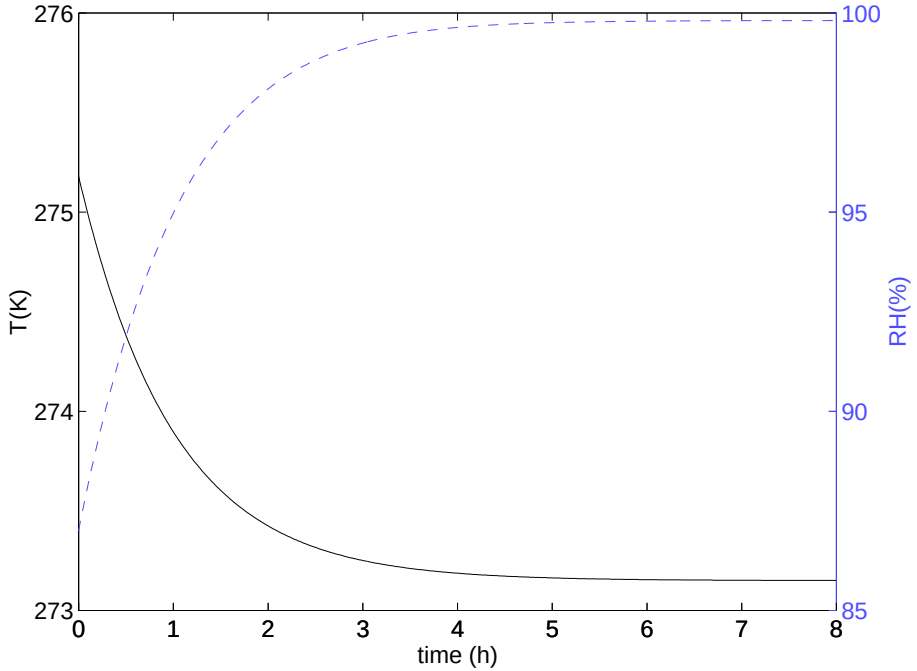

Fig. 1. Relative humidity (dash line) and temperature (solid line) as a function of time for an 8 h run.

ACPD

3, 389–411, 2003

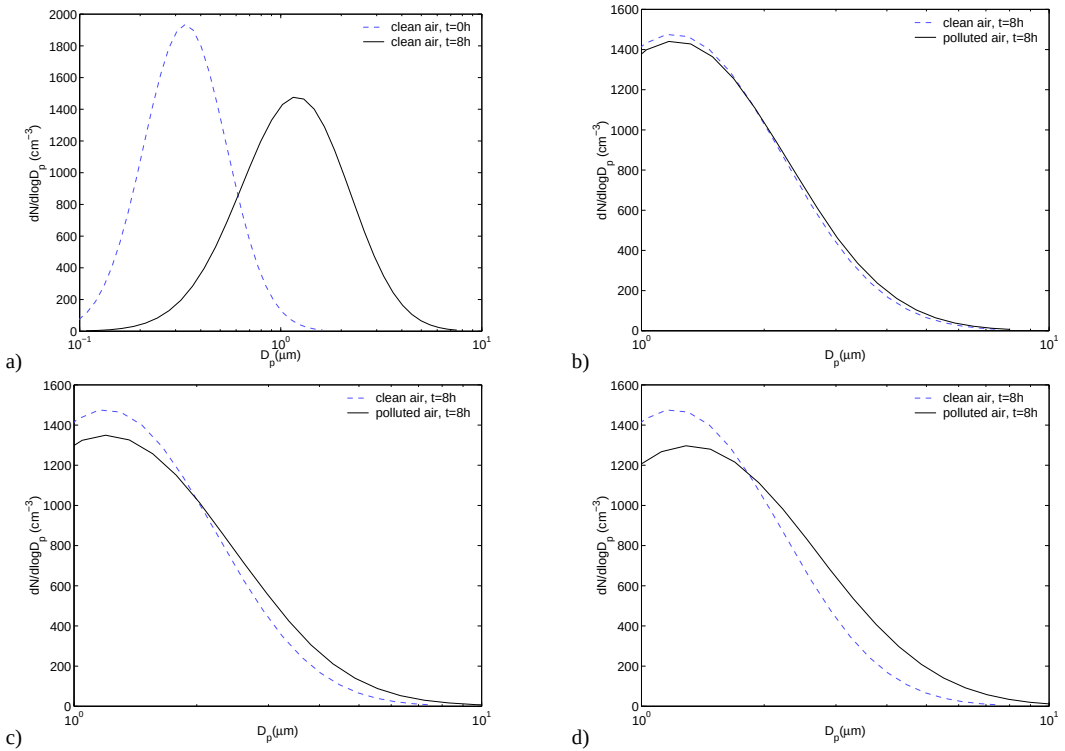

Fig. 2. Number size distribution at t = 0 h (initial) and t = 8 h (final). In (b), (c) and (d) the final number size distributions for the clean air are also included. **(a)** No gaseous pollutants. **(b)** $[SO_2]$= 400 ppb, $[O_3]$= 10 ppb, $[HNO_3]$=0 ppb, $[NH_3]$= 0 ppb. **(c)** $[SO_2]$= 0 ppb, $[O_3]$= 0 ppb, $[HNO_3]$=5 ppb, $[NH_3]$= 10 ppb. **(d)** $[SO_2]$= 400 ppb, $[O_3]$= 10 ppb, $[HNO_3]$=5 ppb, $[NH_3]$= 10 ppb.

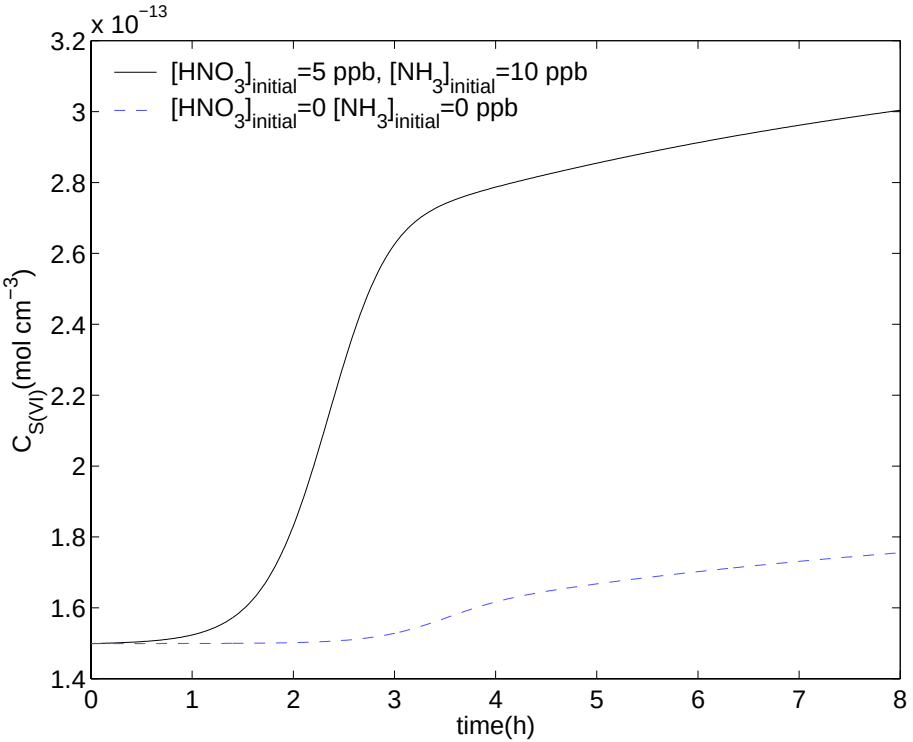

Fig. 3. Sulfate concentration as a function of time.

ACPD
3, 389–411, 2003

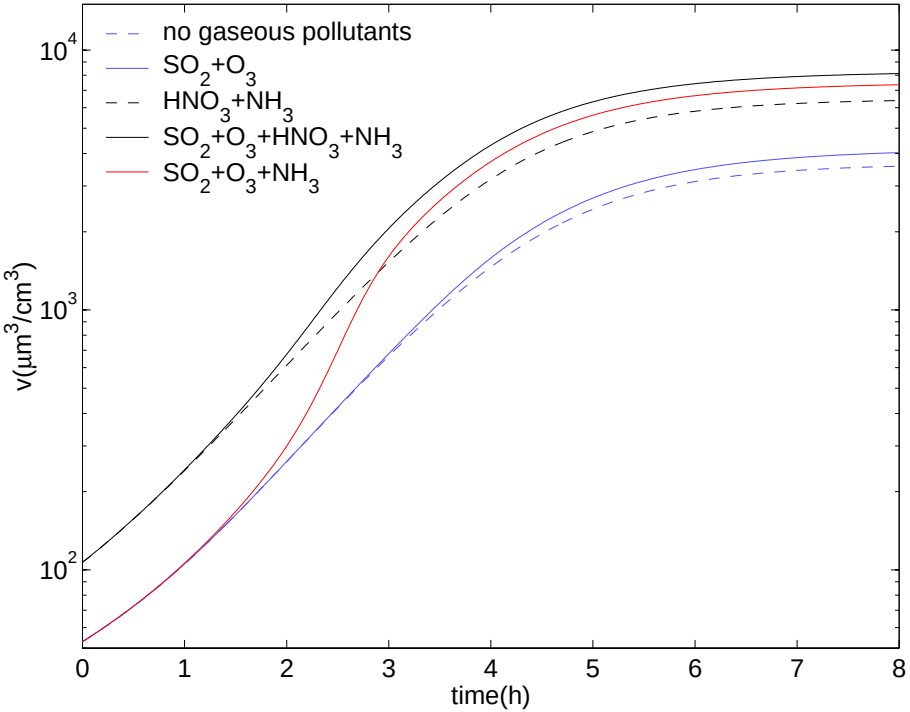

Fig. 4. Total volume concentration of all size bins as a function of time for four different runs.

ACPD
3, 389–411, 2003

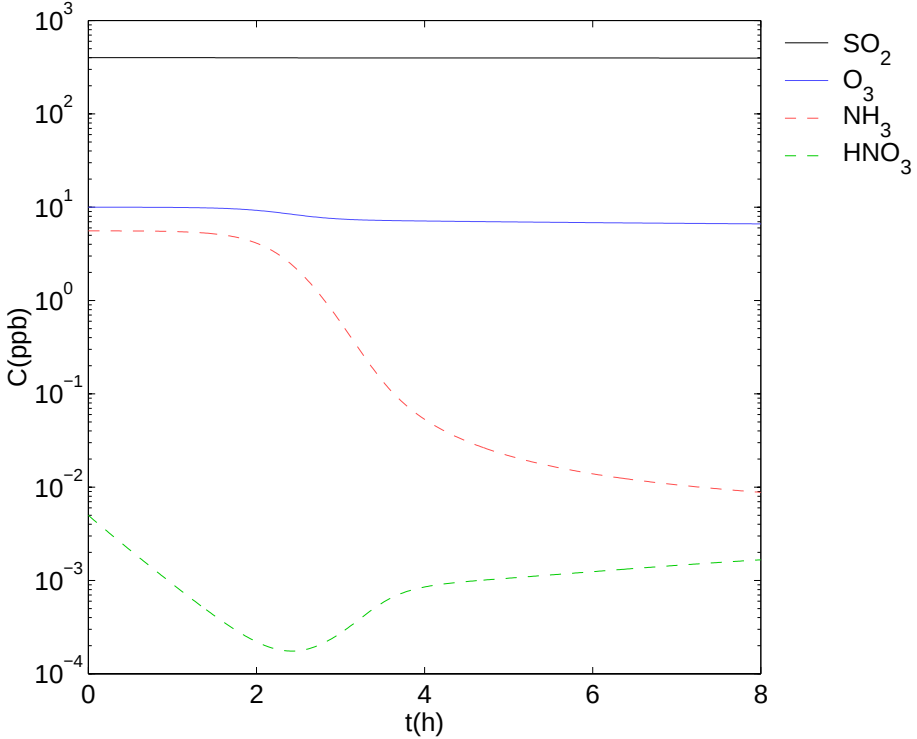

Fig. 5. Gas phase concentrations as a function time.

ACPD

3, 389–411, 2003

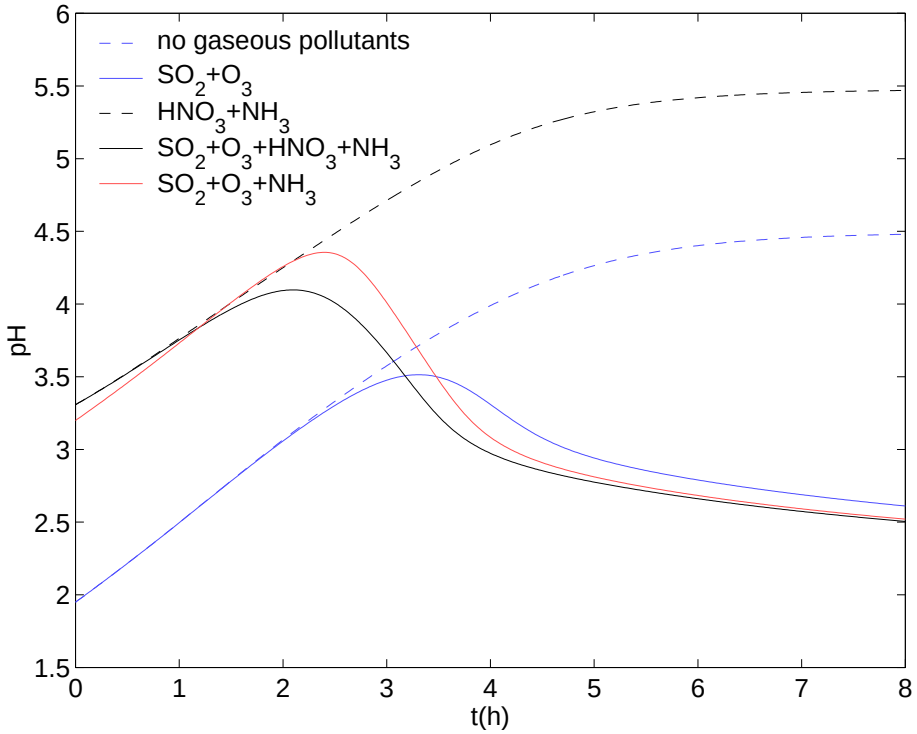

Fig. 6. pH of the largest size bin as a function of time.

ACPD
3, 389–411, 2003

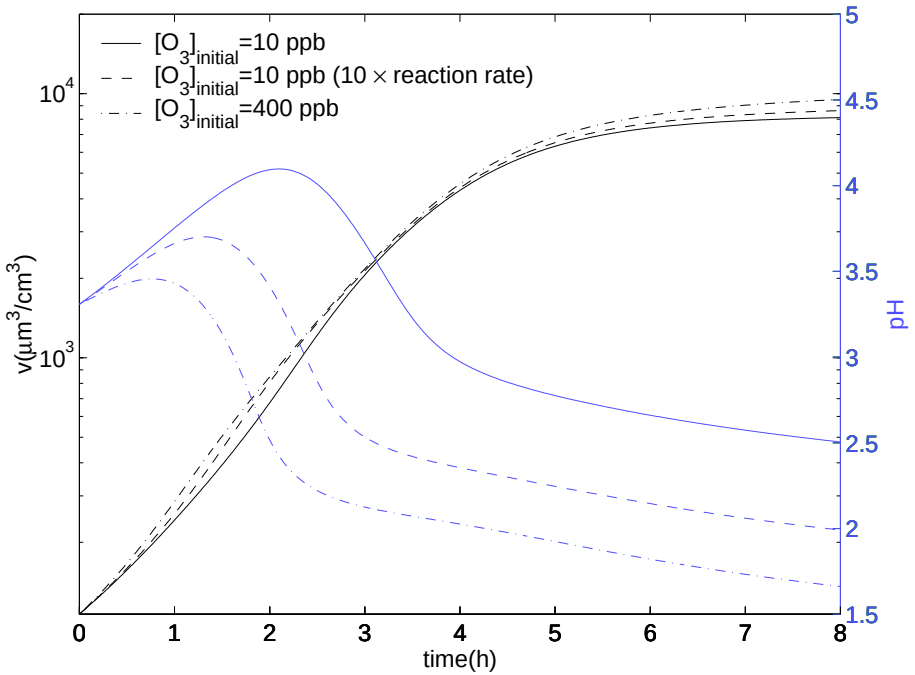

Fig. 7. Total volume concentration of all size bins and the pH of the largest size bin as a function of time for three different runs. Nitric acid and ammonia are present in the system.

ACPD
3, 389–411, 2003

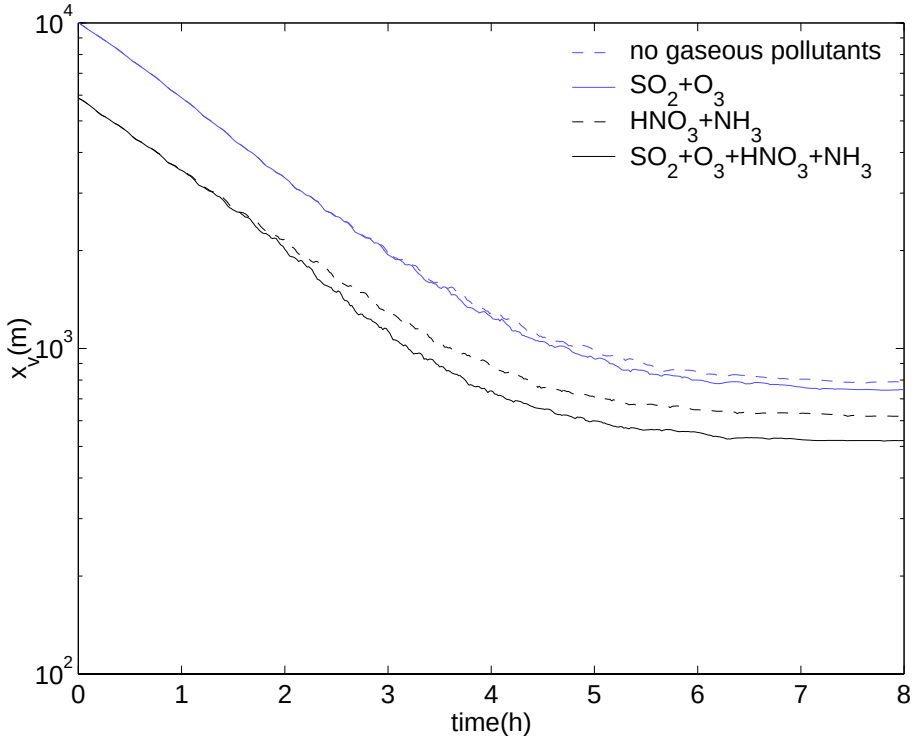

Fig. 8. Visual range x_v as a function of time for four different cases.

ACPD
3, 389–411, 2003